IMPORTANCE OF DEFORMATIONS IN DYNAMICAL EVOLUTION OF PROTON-HALO NUCLEI*

Gudveen Sawhney, Raj K. Gupta

Department of Physics, Panjab University, Chandigarh, India

Manoj K. Sharma

School of Physics and Materials Science, Thapar University, Patiala, India

(Received December 18, 2015)

Based on the cluster–core model, we have extended our recent study on neutron-halo structure of light nuclei to investigate the effects of deformations and orientations on the observed and proposed cases of proton-rich light nuclei. The relevance of "hot compact" over "cold elongated" configurations due to orientations is explored along with the possible role of angular momentum effects. The cases of both $1p$- and $2p$-halo nuclei are analyzed in terms of potential energy surfaces calculated as a sum of binding energies, Coulomb repulsion, nuclear proximity attraction and the centrifugal potential for all the possible cluster+core configurations of a nucleus. The halo structures of ^{11}N and ^{27,28,29}S nuclei are of special interest as they exhibit strong influence of deformations and angular momentum effects.

DOI:10.5506/APhysPolB.47.959

1. Introduction

The study of the properties of light nuclei near the drip lines invokes an important and exciting research topic, which, in turn, contributes immensely towards the overall understanding of nuclear structure and its behavior pattern associated with decay mechanism. The proton- and neutron-rich regimes in the chart of nuclei are characterized by weak binding energies that lead to "exotic" features termed as halos. Most of the halo nuclei are confirmed as neutron halos, since the presence of repulsive Coulomb interaction hinders the formation of a proton halo. So far, the $1p$-halo structures are established for ^{8}B, ^{11}N and ^{17}F and $2p$ halos for only ^{17}Ne, but many more are proposed as the likely candidates.

* Presented at the XXXIV Mazurian Lakes Conference on Physics, Piaski, Poland, September 6–13, 2015.

An appropriate theoretical interpretation is a must for the overall understanding of any physical phenomena, and hence it is worth performing a detailed quantitative or qualitative analysis using a particular approach. In view of this, we have studied [1] the halo structures of a variety of neutron drip-line nuclei at the ground state (temperature $T = 0$), by using the cluster–core model (CCM) [2–4] based on core+valence-nucleons picture. Note, here 'valence nucleons' means the cluster of nucleons forming a halo configuration. The possible role of deformations and associated proximity interactions have been examined in reference to the dynamics of some 24 light neutron-rich nuclei. In order to extend this study further, in the present paper, we apply the same CCM approach to analyze the influence of nuclear deformations and orientations on the core+valence nucleons, *i.e.*, the fragmentation path of both $1p$- and $2p$-halo nuclei, where either the halo structure is already observed or is predicted to be there by some model calculations. This includes the cases of ^{8}B, ^{11}N, ^{12}N, ^{17}F, ^{23}Al, ^{26}P, ^{27}P and ^{28}P (with one-proton halos) and ^{9}C, ^{17}Ne, ^{18}Ne, ^{20}Mg, ^{27}S, ^{28}S, and ^{29}S (with two-proton halos). It is important to mention here that all considered nuclei are deformed, except ^{17}Ne which is spherical, and hence the inclusion of deformation and orientation effects seem desirable, which were not investigated explicitly in the earlier works [2, 3]. In other words, in the present study, we are considering a simple cluster–core picture of light halo nuclei, in terms of the potential energy surfaces, with the idea of learning about their p-halo structure, *i.e.*, we look for a cluster+core configuration with a minimum potential energy (maximum binding energy), which in the language of exotic cluster decay of nuclei [5] means a configuration formed with the largest probability. Of these cluster–core configurations, we concentrate here only on the ones where a cluster of protons is involved. Such a cluster will behave like a proton halo since this is most loosely bound to the core.

Note, the main information regarding the halo structure of a nucleus comes from the separation energy hypothesis. In other words, halo nuclei exhibit low one-proton separation energy $S_{1p}[= B(Z,N) - B(Z-1,N)]$ or two-proton separation energy $S_{2p}[= B(Z,N) - B(Z-2,N)]$, compared to $\sim$ 6–8 MeV/nucleon for stable nuclei. Whereas one-proton halo nuclei exhibit $S_{1p} < S_{2p}$, the two-proton halo nuclei, on the other hand, satisfy $S_{2p} < S_{1p}$. Then, it is of interest to see in what way the angular momentum, and deformation and orientation effects of the decay fragments influence the potential energy surfaces (PES) of these rare light nuclei with p-halo structures. A brief outline of the CCM, with effects of deformations and orientations of nuclei included, is given in Section 2. The results of our calculations for p-halo nuclei are discussed in Section 3, with a summary and conclusions presented in Section 4.

2. The cluster–core model (CCM)

The CCM is based on the well-known Quantum Mechanical Fragmentation theory (QMFT) where the halo nature of a nucleus at the proton drip line is studied via the minimum in fragmentation potential, which, in turn, corresponds to the most probable configuration, *i.e.*, configuration with relatively large preformation probability, compared to its neighbors, for the cluster-decay process. The potential energy for a cluster–core configuration (A_2, A_1) of a nucleus A is defined as the sum of ground-state binding energies, Coulomb interaction, the nuclear proximity, and angular-momentum dependent potentials

$$\begin{aligned} V(A_1, A_2, R, \ell) \; = \; & -\sum_{i=1}^{2} B(A_i, Z_i) + V_{\mathrm{C}}(R, Z_i, \beta_{\lambda i}, \theta_i) \\ & + V_P(R, A_i, \beta_{\lambda i}, \theta_i) + V_\ell(R, A_i, \beta_{\lambda i}, \theta_i) \end{aligned} \quad (2.1)$$

with ground state binding energies Bs taken from the estimates of [6], where the liquid drop model parameters are fitted to experimental Audi–Wapstra [7] or theoretical Möller–Nix [8] tables. The deformation parameters $\beta_{\lambda i}$ of nuclei are also taken from [8]. Thus, shell effects are contained in our calculations that come from the experimental and/or calculated binding energies. The binding energy for a cluster with x protons is defined as

$$B(A_2 = xp) = x\Delta m_p - a_{\mathrm{C}} A_2^{5/3} \quad (2.2)$$

with $\Delta m_p = 7.2880$ MeV, the one-proton mass excess (equivalent of the one-proton binding energy) and Coulomb self-energy constant $a_{\mathrm{C}} = 0.7053$ MeV [9]. The last term in equation (2.2) represents the disruptive Coulomb energy between x protons. In view of our dealing here with light nuclei, only the touching configuration is considered, *i.e.*, $R = R_1 + R_2 = R_t$, with R_i for deformed nuclei, defined as

$$R_i(\alpha_i) = R_{0i}\left[1 + \sum_{\lambda} \beta_{\lambda i} Y_{\lambda}^{(0)}(\alpha_i)\right], \quad (2.3)$$

where $R_{0i} = 1.28A_i^{1/3} - 0.76 + 0.8A_i^{-1/3}$. In above equations, θ_i is the orientation angle between the nuclear symmetry axis and the collision Z-axis, measured in the counter clockwise direction, and α_i is the angle between the symmetry axis and the radius vector $R_i(\alpha_i, T)$ of the colliding nucleus, measured in the clockwise direction from the symmetry axis.

3. Calculations and results

The fragmentation process is studied for 8 cases of 1p-halo nuclei, which include ^{8}B, ^{11}N, ^{12}N, ^{17}F, ^{23}Al, ^{26}P, ^{27}P and ^{28}P and 7 cases of 2p-halo nuclei which include ^{9}C, ^{17}Ne, ^{18}Ne, ^{20}Mg, ^{27}S, ^{28}S, and ^{29}S, covering almost all the known proton-rich nuclei. The calculations have been performed within the framework of CCM for spherical as well as quadrupole deformed (β_2) choices of fragments. Despite the change in PES on inclusion of deformation effects, we find that 1p- and 2p-halo structure remains intact in majority of cases, except for ^{11}N and ^{27,28,29}S nuclei, listed in Table I. The one-proton and two-proton separation energies, S_{1p} and S_{2p}, together with other halo characteristics of ^{11}N and ^{27,28,29}S nuclei are given in Table I. Note that the orientation degree of freedom is fixed by using "optimum" orientation $\theta_i^{\rm opt}$ of Ref. [10] which manifests itself in the form of "hot compact" or "cold elongated" configuration. While the "hot compact" configuration refers to the smallest interaction radius and highest barrier, the "cold elongated" corresponds to the largest interaction radius and lowest barrier. It is relevant to mention here that "optimum" orientations are good only for deformations up to β_2. However, if one is interested in investigating the role of higher-order deformations, then "compact" orientations [11] should be used.

TABLE I

CCM calculated p-halo characteristics of some chosen proton-rich light nuclei. The cluster–core configuration, resulting from the PES, is shown with respect to the $\ell = 0$ case for both the spherical and deformed choices of nuclei.

Nucleus	S_{1p} [keV]	S_{2p} [keV]	Cluster+core configuration referring to PES minimum: Spherical nuclei	Deformed nuclei
^{11}N	−2046.3	−114.5	$1p+^{10}$C/$3p+^{8}$Be	$1p+^{10}$C/$3p+^{8}$Be
^{27}S	1152.7	−1060.1	$1p+^{26}$P	$2p+^{25}$Si
^{28}S	2187.8	1286.9	$1p+^{27}$P	$2p+^{26}$Si
^{29}S	3390.6	1060.3	$2p+^{27}$Si	$2p+^{27}$Si

Figure 1 (a) presents a comparative analysis of the two configurations ("hot compact" or "cold elongated") for the case of ^{8}B halo nucleus. We find here a clear preference for "hot compact" configuration. In view of this observation, in the following, we use this prescription of "hot compact" configurations for any further investigation of p-halo structure of nuclei.

Figures 1 (b) and 1 (c) illustrate the fragmentation potentials for ^{11}N nucleus calculated for the spherical and β_{2i} deformed cases of nuclei. Both $\ell = 0$ and an arbitrary $\ell = 2$, 4 ($\hbar$) values are considered for the angular

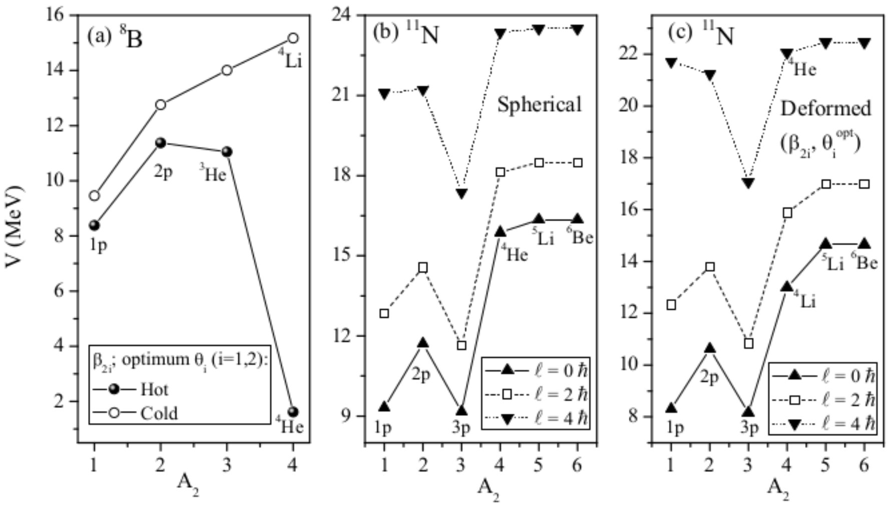

Fig. 1. Fragmentation potential for (a) ^{8}B at $\ell = 0$ for deformed nuclei with "optimum" $\theta_i^{\rm opt}$, forming "hot" or "cold" configuration. Panels (b) and (c) are for ^{11}N nucleus, plotted at different ℓ values for both the spherical and deformed (β_{2i} alone) cases, having 'hot optimum' choice of configuration.

momentum part of the potential V_ℓ in Eq. (2.1). In general, both the positions and depths of potential energy minima in $V(A_2)$ are found [12] to be nearly independent of the contribution of ℓ-dependent term in it. Interestingly, for the case of ^{11}N, we find that 1p+core minimum is almost as deep as for 3p+core configuration at $\ell = 0$, irrespective of the choice of shape (spherical or deformed choice of nuclei). However, the most probable cluster configuration gradually changes to 3p-halo structure with the increase in ℓ value which signifies the angular momentum ℓ effects in context of the halo nature of this nucleus. This effect may correspond to the mixed angular momentum (and parity) states for the ground state configuration [13]. Hence, in the following, we discuss only $\ell = 0$ configuration. Also, S_{3p} ($= -2619.2$ keV) comes out to be comparable with S_{1p} ($= -2046.3$ keV). Apparently, further experiments and calculations are necessary for the halo status of ^{11}N nucleus.

Next, the study of $^{27-29}$S nuclei in Fig. 2 is of extreme relevance and interest here, as it gives 2p halo for the choice of deformed (β_{2i}) case, though the PES for spherical configuration suggests the emergence of 1p-halo structure together with the expected 2p-halo. Also, we notice from Table I that S_{2p} is lower than S_{1p} for all the ^{27,28,29}S systems, which suggests that they are all 2p-halo nuclei. Thus, deformation and orientation effects up to quadrupole (β_{2i}) deformations seem indispensable for the case of 2p-halo systems.

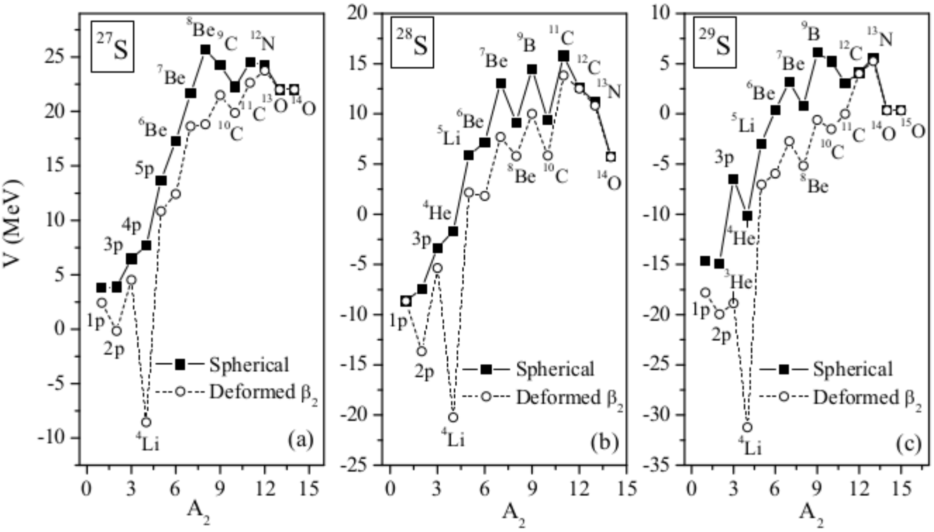

Fig. 2. Fragmentation potential for (a) ^{27}S, (b) ^{28}S and (c) ^{29}S nuclei, taking the two fragments as spheres or with β_{2i} deformations, at $\ell = 0$.

4. Summary and conclusions

Summarizing, the present study points out the significance of deformation effects, specifically for ^{11}N and ^{27,28,29}S proton-rich nuclei. The behavior of PES is investigated in order to extract a better picture of the dynamics involved. The angular momentum effects are also explored for one illustrative case of ^{11}N, using both approaches of spherical and deformed configurations. As an extension of this work, it will be of interest to look for the exclusive role of a variety of nuclear interaction potentials, for a further description of proton-halo structure.

Financial support from the University Grants Commission (UGC) in the form of Dr. D.S. Kothari Fellowship (F.13-901/2013(BSR)) and Council of Scientific and Industrial Research (CSIR) under Major Research Project (03(1341)/15/EMR-II) is gratefully acknowledged.

REFERENCES

[1] G. Sawhney, M.K. Sharma, R.K. Gupta, *J. Phys. G: Nucl. Part. Phys.* **41**, 055101 (2014).

[2] R.K. Gupta, M. Balasubramaniam, R.K Puri, W. Scheid, *J. Phys. G: Nucl. Part. Phys.* **26**, L23 (2000).

[3] R.K. Gupta *et al.*, *J. Phys. G: Nucl. Part. Phys.* **28**, 699 (2002).

[4] R.K. Gupta *et al.*, *J. Phys. G: Nucl. Part. Phys.* **32**, 565 (2006).

[5] S.S. Malik, R.K. Gupta, *Phys. Rev. C* **39**, 1992 (1989).

[6] B.B. Singh, M.K. Sharma, R.K. Gupta, *Phys. Rev. C* **77**, 054613 (2008).

[7] G. Audi, A.H. Wapstra, C. Thibaul, *Nucl. Phys. A* **729**, 337 (2003).

[8] P. Möller, J.R. Nix, W.D. Myers, W.J. Swiatecki, *At. Nucl. Data Tables* **59**, 185 (1995).

[9] W.D. Myers, W.J. Swiatecki, *Nucl. Phys.* **81**, 1 (1966).

[10] R.K. Gupta *et al.*, *J. Phys. G: Nucl. Part. Phys.* **31**, 631 (2005).

[11] R.K. Gupta, M. Manhas, W. Greiner, *Phys. Rev. C* **73**, 054307 (2006).

[12] D.R. Saroha, N. Malhotra, R.K Gupta, *J. Phys. G: Nucl. Phys.* **11**, L27 (1985).

[13] H. Simon *et al.*, *Phys. Rev. Lett.* **83**, 496 (1999).